Axial channelling of low-energy antiprotons

1992 J. Phys.: Condens. Matter 4 4883

(http://iopscience.iop.org/0953-8984/4/21/004)

J. Phys.: Condens. Matter 4 (1992) 4883–4893. Printed in the UK

Axial channelling of low-energy antiprotons

L L Balashova†, N M Kabachnik†, V I Shulga† and Ch Trikalinos‡

† Institute of Nuclear Physics, Moscow State University, Moscow 119899, Russia

‡ University of Athens, Physics Department, Panepistimioupoli-Kouponia, 157 17 Athens, Greece

Received 23 July 1991, in final form 3 February 1992

Abstract. Monte Carlo computer simulation of the passage of antiprotons and protons through a silicon crystal under axial channelling conditions is performed. The energy spectra and angular distribution of channelled protons and antiprotons moving along the ⟨110⟩ direction are calculated and compared. The projectile energy range is from 300 keV to several megaelectronvolts. It is shown that the energy loss corresponding to the maximum of the antiproton spectrum is close to the energy loss of particles moving in a random direction. Moreover, the most probable energy loss of the channelled part of the antiproton beam is slightly less than the random energy loss. The Barkas correction to the energy loss has little effect on the energy spectra of channelled particles and can hardly be studied with this type of experiment. The angular distributions of protons and antiprotons differ considerably. The characteristic features of the angular distribution may serve as evidence of channelling of low-energy antiprotons.

1. Introduction

The channelling effects in particle penetration through crystalline solids were widely studied for heavy positively charged projectiles in the low-energy region (less than 10 MeV/nucleon) [1]. Various directional effects in a single-crystal material have been observed and discussed for relativistic electrons and positrons [1, 2] and for a variety of very energetic (above 1 GeV heavy particles with both positive and negative charges (see, e.g. [3], and references therein)). Considerably less is known about channelling of heavy negative particles in the low- and intermediate-energy region. Although some experiments were performed with negative mesons [4] a systematic study of the channelling characteristics of negative heavy particles with low energies is still lacking. New experimental possibilities arising from the use of low-energy antiproton facilities of LEAR in CERN [5, 6] led to a revival of interest in this problem. Channelling of antiprotons has been theoretically considered in [7–9]. In the report by Balashova *et al* [7], energy spectra of antiprotons transmitted through a thin crystalline foil were calculated. It was shown that the position of the maximum of the antiproton energy spectra in the channelling regime is close to that in the random case. However, the shapes of the spectra are different. In the antiproton spectrum a group of particles having greater energy loss than that for the random case is formed. This group consists of particles moving along finite (spiralling) trajectories with large eccentricty. Such particles periodically approach an atomic row closely and deeply penetrate into the region of high energy losses owing to the core electrons. This result was obtained using a rather crude model without taking into account the multiple scattering and

0953-8984/92/214883+11$04.50

thermal motion of the atoms. It was not clear whether these features of the spectrum would be conserved in a more realistic model.

Another problem is the effect of the so-called Z_1^3 or Barkas corrections to the energy loss. It was shown recently [10, 11] that the charge asymmetry effects are rather strong in the impact parameter dependence of energy loss at least for low-energy projectiles ($E < 1$ MeV). In principle these effects can influence the energy loss in channelling. A study of the particle stopping in the channelling regime is a well known means of investigating the impact parameter dependence of energy losses [12, 13]. The question arises of whether it is possible to study the impact parameter dependence of the Z_1^3 corrections by measuring the energy losses of channelled protons and antiprotons. As was discussed in [7] the difference between the energy spectra of channelled protons and antiprotons is rather strong owing to the pure kinematic factors associated with the repulsive (attractive) character of the proton (antiproton) interaction with atomic rows or planes. Thus a comparatively weak dynamic Z_1^3 effect may be masked by a stronger kinematic difference.

The purpose of the present paper is to analyse the energy distribution of low-energy antiprotons moving under axial channelling conditions in a single crystal using the Monte Carlo simulation method with a realistic model of particle motion in a crystal. We have also studied peculiarities of the angular distribution of antiprotons transmitted through a crystal. One of the problems that will be discussed in the paper is the search for experiments which could provide proof of the existence of the channelling phenomenon for low-energy antiprotons.

2. Calculation procedure

In order to calculate the energy spectra of axially channelled antiprotons we use the Monte Carlo computer simulation of individual particle trajectories. A detailed description of the computer program ASTRA as well as the basic physical assumptions used in the calculation were given in [14]. Here we briefly discuss the main characteristics of the model.

The crystal was treated as a set of static atomic strings according to the Lindhard's [15] model for axial channelling. The individual particle trajectories were calculated by solving numerically the classical equation of motion in the force field of the surrounding atomic strings and taking into account the inelastic stopping by the target electrons. The force of the elastic interaction was calculated using the Moliere–Erginsoy potential [16]:

$$U(r) = \frac{Z_1 Z_2 e^2}{d} \sum_{i=1}^{3} \alpha_i K_0\left(\frac{\beta_i r}{a_s}\right) \qquad (1)$$

where r is a distance from an atomic row, $Z_1 e$ and $Z_2 e$ are the nuclear charges of incident particles and target atoms, respectively, d is the spacing between the nearest atoms in the string, a_s is the Thomas–Fermi screening radius, $\{\alpha_i\} = 0.1$, 0.55 and 0.35 and $\{\beta_i\} = 6$, 1.2 and 0.3 for $i = 1$, 2 and 3, respectively, and $K_0(x)$ is the modified Bessel function of the second kind of zero order. In our case, $Z_1 = 1$ and -1 for protons and antiprotons, respectively. We assumed that including the thermal vibration of target atoms leads to the fluctuation of the elastic force which is [17]

$$\delta F^2 = (u_1^2/2)[F'^2 + (F/r)^2] + (u_1^2/2)^2[\tfrac{3}{4}(F^2/r^4) - \tfrac{1}{2}(FF'/r^3) - \tfrac{1}{4}(F'/r)^2 + \tfrac{1}{2}(FF''/r^2) + \tfrac{3}{2}(F'F''/r) + \tfrac{3}{4}(F'')^2 + F'F'''] \qquad (2)$$

where $F = F(r)$ is the elastic force, $F' = \mathrm{d}F/\mathrm{d}r$, $F'' = \mathrm{d}^2F/\mathrm{d}r^2$, $F''' = \mathrm{d}^3F/\mathrm{d}r^3$ and u_1 is the amplitude of thermal vibrations in two dimensions†.

The multiple scattering of moving particles on target electrons was taken into account. The scattering was considered to be isotropic in the azimuthal angle. The polar angle of scattering was assumed to be normally distributed with the mean square deviation determined as [17]

$$\langle\Theta^2\rangle = \tfrac{1}{2}(m/M)\Delta E/E. \tag{3}$$

Here m is the electron mass, M is the penetrating particle mass, E is the particle energy and ΔE is the energy loss at the integration step.

The dechannelling process was taken into account by assuming that a particle is dechannelled if its distance to the atomic string is smaller than the critical distance $r_c = u_1$.

To calculate the energy loss of a channelled particle we used a model which successfully described the experimental data on the energy loss of the axially channelled protons [14]. We assume that the contributions to the stopping power from valence and core electrons are independent:

$$S_e(r) = S_{val}(r) + S_{core}(r). \tag{4}$$

The stopping power due to valence electrons was calculated using the expression suggested by Lindhard [15]:

$$S_{val}(r) = (4\pi Z_1^2 e^4/mv^2)\, Z_{val}[(1-\alpha) + \alpha\rho(r)]L_e \tag{5}$$

where v is the projectile velocity, Z_{val} is the number of valence electrons per atom, $\rho(r)$ is the relative local valence electron density averaged over the corresponding channel direction and L_e is the stopping number: $L_e = \ln(2mv^2/\hbar\omega_p)$, where ω_p is the plasma frequency depending on the mean valence electron density. The coefficient α describes that part of close collisions which, according to Lindhard's model, is proportional to the electron density. As was shown in [14] for the considered energy range the best agreement with experiment was obtained when $\alpha = 0.5$ which is consistent with Bohr's [18] equipartition rule.

The valence electron density averaged over the corresponding channel direction was calculated using the Fourier analysis of x-ray diffraction experiments [19]. To calculate the stopping number L_e we used the expressions obtained by Lindhard and Winther [20] for a homogeneous electron gas with a mean plasma frequency.

The contribution of the core electrons to stopping power was calculated by the summation of contributions of the surrounding atomic strings:

$$S_{core}(r) = \frac{1}{N}\sum_j \frac{\Delta E(r_j)}{d} \tag{6}$$

where N is the atomic density of the target and r_j is the distance between the projectile and the jth string in the transverse plane. The mean energy loss to core

† There is a misprint in the second term in square brackets in equation (1.29) of [16], for the value of δF^2.

electrons of an individual atom at a given impact parameter $\Delta E(r_j)$ was calculated in terms of the semiclassical approximation [21].

In order to study the influence of the charge asymmetry effects in stopping power (Z_1^3 or Barkas effect) on the spectra of channelled protons and antiprotons, we added the so-called Z_1^3 corrections to $S_e(r)$. For core electrons, $S_{core}(r)$ was calculated with allowance for binding and Coulomb deflection [10]. For valence electrons we used the approximate form suggested by Sung and Ritchie [22] and so L_e in (6) was substituted by

$$L_e' = L_e[1 + Z_1(8\pi/10)(e^2\omega_p/v^3)]. \tag{7}$$

These corrections lead to a slightly different local stopping power for protons and antiprotons. As was shown in [11] the difference may be large at comparatively small energies (about 100 keV) and decreases with increasing energy. It is almost negligible at energies higher than 1 MeV.

The energy loss of dechannelled particles from the point of dechannelling to the exit from the crystal was calculated using the stopping cross section for a random motion which was obtained by averaging the value $S_e(r)$ over the channel.

3. Results and discussion

The calculations were performed for protons and antiprotons moving along the ⟨110⟩ direction of the silicon single crystal in the energy interval 0.3–4 MeV. We calculated both the energy spectra of the transmitted particles and their angular distribution. In all cases, 1000–1500 particles were involved.

First consider typical trajectories of protons and antiprotons in the case of axial channelling. Figure 1 shows some examples of the calculated trajectories projected onto a plane perpendicular to the channel direction. As is well known the channelled proton motion in the transverse space may be confined to one or two channels formed by the atomic rows (figures 1(*d*) and 1(*e*)) or the protons may wander among adjacent channels as in figure 1(*f*). In all cases their trajectories stay far away from the strings of atoms. Negative particles are attracted by the negative string potential therefore their trajectories may come much closer to the string (figure 1(*c*)). Besides, as was discussed in [3, 7], negative particles can establish trajectories that spiral around atomic rows. Figures 1(*a*) and 1(*b*) show examples of such a spiralling rosette motion of antiprotons around one and two axes. The spiralling motion is disturbed by the multiple scattering on electrons and nuclei. However, even with these factors taken into account the results of our calculations suggest that there is a noticeable probability for antiprotons to be captured into rather stable spiral-type trajectories.

3.1. Energy spectra of channelled particles

In figures 2 and 3 we present the calculated energy spectra for 300 keV protons and antiprotons transmitted through a silicon crystal 1000 Å thick. The incidence angle relative to the ⟨110⟩ axis is $\psi_{in} = 0.4\psi_c$ (figure 2) and $0.1\psi_c$ (figure 3) where ψ_c is the Lindhard critical angle:

$$\psi_c = \sqrt{2Z_1Z_2e^2/dE}. \tag{8}$$

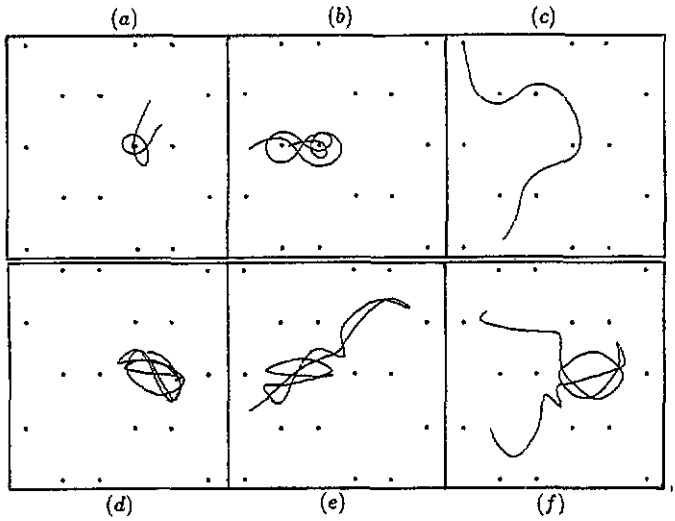

Figure 1. Typical calculated trajectories of (*a*)–(*c*) channelled antiprotons and (*d*)–(*f*) channelled protons projected onto the plane transverse to the atomic rows which are indicated by points. $E_0 = 300$ keV; crystal thickness, 500–1000 Å.

In the considered case, $\psi_c = 1.072°$. The azimuthal angle of incidence was chosen to be $\varphi = 29°$ from the x axis (see inset in figure 6 later). This angle does not correspond to any low-index planar direction in the crystal. The angular spread of the primary beam was taken into account by adding the Gaussian distribution of incidence angles with the width $\sqrt{g^2} = 0.1\psi_c$ which is typical for channelling experiments. All particles transmitted through crystal were included in spectra. The arrows in the figures indicate the energy loss corresponding to the random case. The shaded part of the histogram shows the contribution of 'channelling' antiprotons which are defined as passing through the whole crystal in the channelling regime (without dechannelling).

It can be seen from the figure that the energy spectra of protons and antiprotons differ considerably. Whereas the channelled proton stopping is significantly less than the stopping in the random case, the most probable energy loss of antiprotons is almost the same as the energy loss in the random case. The shapes of the spectra are also different. The antiproton spectrum is wider and has a high-loss tail which is absent in the case of protons. According to our previous calculations [7] this tail may be attributed to the particles which spent considerable time moving along spiralling trajectories with large eccentricity (see figure 1). Such particles pass the region near the string with large electron density. The energy losses of such particles are greater than in the random cases. However, these particles have a large probability of being scattered violently and therefore of being dechannelled. One can see that in fact this part of the spectrum consists mainly of dechannelled antiprotons. Those antiprotons that pass the whole crystal in the channelling regime have energy loss slightly less than in the random cases but greater then for channelled protons.

In order to explain the difference between the energy losses suffered by channelled protons and antiprotons it is instructive to consider the spatial distribution of the flux density $\Phi(x, y)$ in the plane perpendicular to the $\langle 110 \rangle$ axis which is displayed in figure 4. The figure shows a remarkable difference between the proton and antiproton

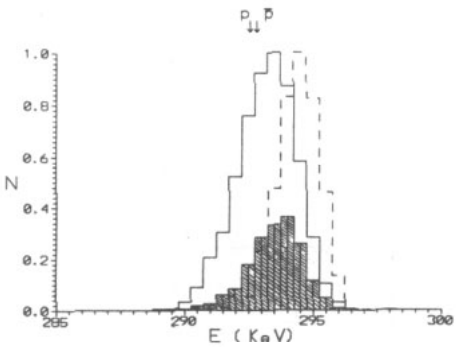

Figure 2. The calculated energy spectra of the 300 keV antiprotons (—) and protons (- - -) transmitted through a silicon crystal 1000 Å thick along the ⟨110⟩ axes. Both spectra are normalized to unity at the maximum. The incident angle is $\psi_{in} = 0.4\psi_c$. The arrows indicate the most probable energy losses corresponding to a random direction of motion. The shaded area shows the fraction of the channelled antiprotons. $f_{ch} = 0.31$.

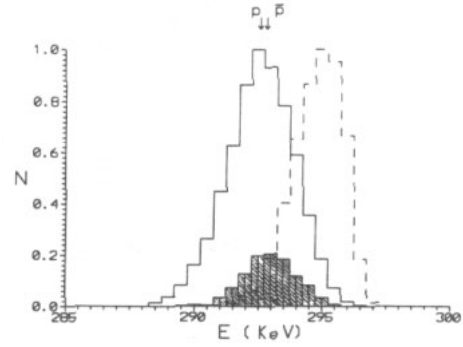

Figure 3. The same as in figure 2 but for $\psi_{in} = 0.1\psi_c$. $f_{ch} = 0.17$.

distributions. The antiprotons are distributed much more uniformly than protons. Although the flux density of antiprotons slightly increases towards the strings (sharp minimum at the string position is connected with the cut-off radius r_c in our model), only a small fraction of the flux is concentrated near the strings where the energy loss is larger than in the random cases. The majority of antiprotons are almost uniformly distributed across the channel and have almost the same average energy loss as those moving in a random direction. On the contrary, protons are strongly concentrated near the centre of the channel (point A) in the region of decreased electron density. Therefore on average their energy losses are lower than in the random cases.

A difference between the flux densities of protons and antiprotons in the vicinity of strings results in a much stronger dechannelling effect for antiprotons and eventually in a considerable decrease in the channelled antiproton transmission probability. The latter may be characterized by the fraction $f_{ch} = N_{ch}/N_{tot}$ of the channelled particles at the exit from the crystal (this fraction is given by the ratio of the shaded area to the total area under the histogram in figures 2 and 3). It is clear from figures 2 and 3 that the channelled fraction strongly depends on the incidence angle. A detailed study of the transparency coefficient of thin crystals for antiprotons as well as a study of the axial-to-planar channelling transition is in progress.

As was mentioned in section 1, there are two types of factor which are responsible for the difference between the energy spectra of channelled positive and negative particles, namely the purely kinematic factor and the dynamic Z_1^3 or Barkas effect in the impact parameter dependence of energy loss. In order to estimate the influence of the Barkas effect we calculated the energy loss spectra excluding the Z_1^3 corrections. The result of the calculation almost coincides with the previous result where the corrections were included. Therefore we may conclude that the influence of the Barkas effect is too small and in energy loss spectra the difference between protons and antiprotons due to charge-asymmetry effects is strongly masked by the much

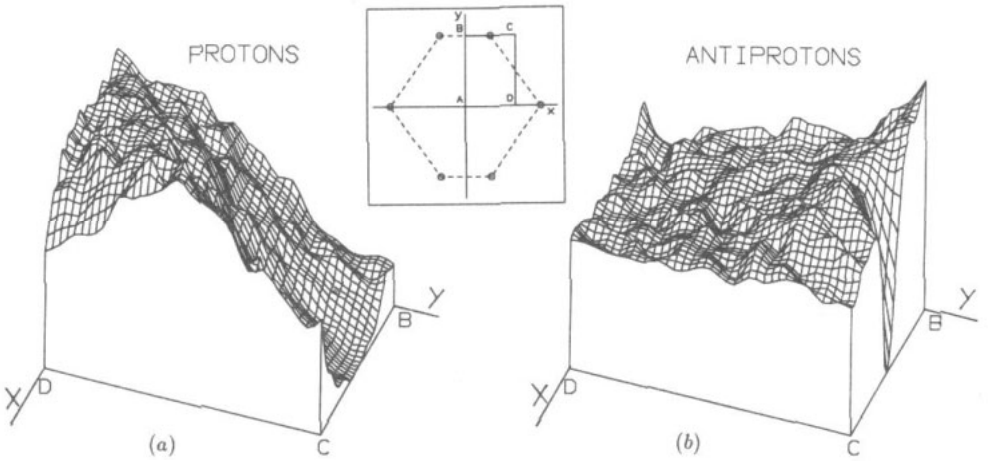

Figure 4. The flux density distribution for protons and antiprotons onto the plane transverse to the ⟨110⟩ channel of the Si crystal at a depth of 1000 Å. In the inset the chosen framework is shown and the part of the channel displayed in the figure is indicated. The open circles indicate atomic rows, the x axis indicates the (001) plane and the y axis indicates the $(1\bar{1}0)$ plane.

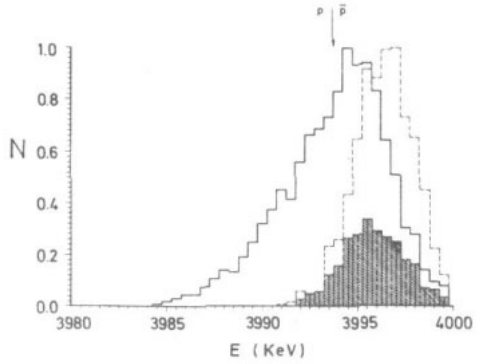

Figure 5. The calculated spectra of the 4 MeV antiprotons and protons transmitted through a silicon crystal 5000 Å thick along the ⟨110⟩ axis. The incidence angle is $\psi_{in} = 0.4\psi_c$. The notation is the same as in figure 2.

larger difference due to the purely kinematic effect.

In figure 5 we show the calculated energy spectra for 4 MeV protons and antiprotons after passing a 5000 Å Si foil in the same conditions as above. As we can see, these spectra have the same character as for 300 keV and all the above-mentioned conclusions are valid for higher energies as well. The difference between the shapes of the spectra is even more pronounced here than at lower energies. The difference between protons and antiprotons is completely determined by the kinematics of particle motion. The Z_1^3 corrections in this energy region are negligible.

As was shown in [23] the energy spectra of channelled negative particles strongly depend on experimental cuts in both incident and exit angular distributions. Similar investigations are in progress.

3.2. Angular distribution of channelled particles

One of the well known manifestations of the channelling phenomenon is the angular

distribution of particles transmitted through a crystal along one of the crystalline axes. In the energy region discussed, behind a sufficiently thick crystal, heavy positively charged particles form characteristic 'star' patterns [1]. In thin (less than 1 nm) crystals the angular distribution shows a typical ring-shaped pattern with an anisotropic azimuthal distribution. This pattern is explained by the conservation of the transverse energy in particle scattering from a string and it has been comprehensively studied both experimentally and theoretically [24–32]. It is interesting to compare the angular distribution of protons and antiprotons transmitted through a silicon crystal 1000 Å thick along the ⟨110⟩ axis. The initial energy is 300 keV and the incidence angle relative to the axis is $\psi_{in} = 0.4\psi_c$, $\varphi = 29°$. The proton angular distribution (figure 6(*a*)) shows a ring-shaped pattern around the considered axis with a strong azimuthal anisotropy. When the incidence angle is less than the critical angle, the radius of the ring (in angular units) corresponds approximately to the angle between the beam direction and the axial direction of the target crystal. A sharp maximum corresponds to the original beam direction.

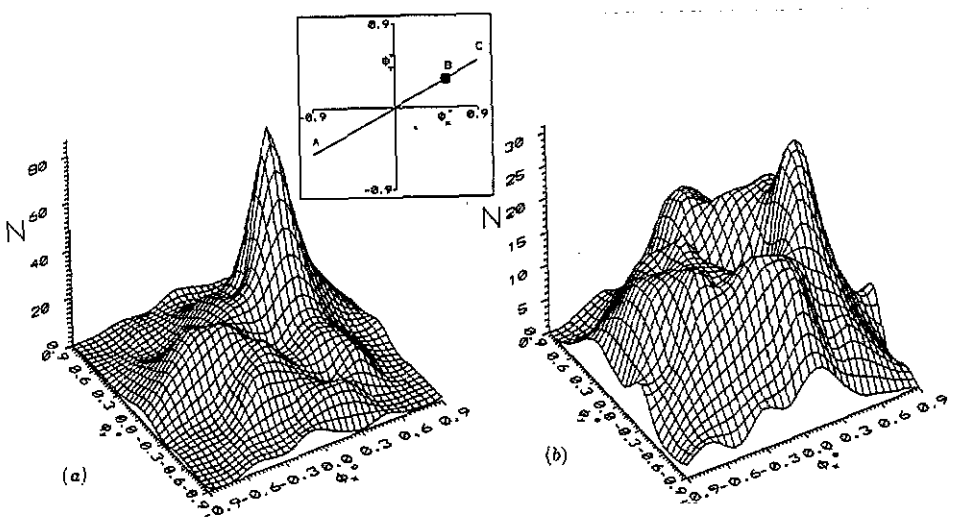

Figure 6. The relative intensity distribution of (*a*) the 300 keV protons and (*b*) the 300 keV antiprotons transmitted through a 1000 Å Si single crystal as a function of the angle between the ⟨110⟩ axis and the exit direction. The incidence angle $\psi_{in} = 0.4\psi_c$. The inset shows the initial beam orientation B. Φ_x is the angle between the particle and the $(1\bar{1}0)$ plane; Φ_y is the angle between the particle and the (001) plane. The (0,0) direction is parallel to the ⟨110⟩ axis.

A different picture has been obtained for antiprotons (figure 6(*b*)). Here the ring-shaped distribution is also formed; however, the azimuthal anisotropy is considerably less than in the proton case. The initial beam direction is virtually 'forgotten' and the angular distribution is almost axially symmetric. The remaining azimuthal anisotropy is due to the blocking effect in directions of other low-index crystalline axes. Similar results have been obtained for channelled 15 MeV electrons [31].

A drastic difference between the proton and antiproton angular distributions is clearly seen in the sections of the discussed distributions by the plane comprising the incident beam direction and the atomic row (figure 7). The intensities in the direction of the incident beam and in the direction of 'mirror' reflection differ considerably in

the proton case while for antiprotons both maxima are almost equal. A similar symmetrical picture could be formed with protons but in a substantially thicker crystal. To explain the observed difference consider again the flux density distribution of particles in the crystal (figure 4). On average, protons move farther away from the atomic rows than antiprotons do. Therefore they suffer less multiple scattering on electrons and nuclei and less effective scattering from strings. The process of reaching statistical equilibrium in transverse momentum is faster for antiprotons than for protons. This leads to a more symmetric pattern of the angular distribution of antiprotons. Similar problems have already been discussed for gigaelectronvolt protons, π^+ and π^- mesons [3] and megaelectronvolt positrons and electrons [31, 32]. Here it was observed that the tendency towards equilibrium in transverse momentum is stronger for negative than for positive relativistic particles. The qualitative explanation of this fact was given using the theory developed in [29]. Our calculations predict that this effect is very strong in the low-energy region.

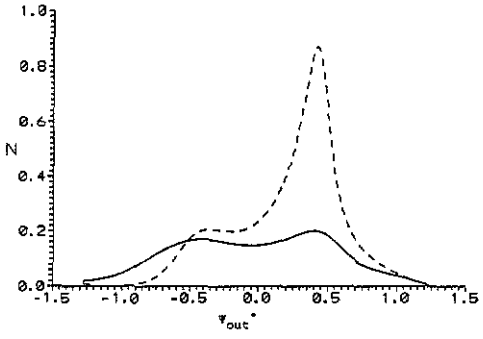

Figure 7. Scan through the distributions shown in figure 6 (the scan direction is along the ABC line in the inset). Relative intensities of antiprotons (—) and protons (- - -) are shown as functions of the angle ψ_{out} between the axis (0°) and the exit direction.

As we have already mentioned, one of the important problems in the channelling of low-energy heavy negative particles is a search for an experimental means of revealing the channelling phenomenon itself. As we have seen in the previous section the energy spectra are hardly appropriate for this purpose because the energy loss of the channelled antiprotons is close to the value for the random case. The problem is even more complicated since the dechannelling length for antiprotons is less than for protons. Therefore the beam of particles transmitted through even a thin crystal contains a large number of dechannelled antiprotons. From the results discussed earlier, it follows that the angular distribution of antiprotons in thin crystal should reveal the pattern typical for channelling; thus it can be used as evidence of the channelling itself. This conclusion is in accordance with the experimentally observed 'steering' effect for intermediate-energy negative pions under axial channelling conditions [4].

4. Conclusions

We have studied theoretically the passage of low-energy antiprotons through a single crystal under axial channelling conditions. We used a Monte Carlo computer simulation method based on a realistic model including multiple-scattering, straggling and dechannelling effects. A rather sophisticated model of energy losses was used in order to reproduce properly the energy spectra of channelled particles. Special

attention was paid to the influence of the Z_1^3 or Barkas correction to the energy loss which causes the difference between the energy losses for protons and antiprotons in a single collision with an atom.

The calculations show that the energy spectra of antiprotons and protons transmitted along a crystalline axis are different. The antiproton spectrum is wider and has a high-loss tail. However, the most probable energy loss for antiprotons in the aligned case is close to the random value. Thus observing the antiproton channelling effect by energy spectrum measurements is questionable. In this respect more favourable conditions may be provided by measurements of angular distribution patterns in thin crystals. The antiproton angular distribution shows a characteristic ring-shaped pattern around the axis direction. It is more axially symmetric than the corresponding proton angular distribution. The angular distribution measurements may provide proof of the existence of channelling for antiprotons. The dynamic difference between the stopping of protons and that of antiprotons (charge-asymmetry effect in a single collision) is strongly masked by the pure kinematic difference. Thus it seems very difficult, if not impossible, to obtain information about the Z_1^3 effects in stopping from channelling experiments.

References

[1] Gemmell D S 1974 *Rev. Mod. Phys.* **46** 129
[2] Beloshitsky V V and Trikalinos Ch G 1981 *Radiat. Eff.* **56** 71
[3] Andersen S K, Fich O, Nielsen H, Schiott H E, Uggerhoj E, Vraast Thomsen C, Charpak G, Petersen G, Sauli F, Ponpon J P and Siffert P 1980 *Nucl. Phys.* B **167** 1
[4] Gemmell D S, Holland R E, Pietsch W J, Ratkowski A J, Schiffer J P, Wangler T P, Worthington J N, Zeidman B, Morris C L and Thiessen H A 1981 *Proc. 7th Int. Conf. on Atomic Collisions in Solids (Moscow, 1977)* (Moscow: Moscow State University Publishing House) p 128
[5] Uggerhoj E 1988 *Nucl. Instrum. Methods* B **33** 265
[6] Moller S P 1990 *Nucl. Instrum. Methods* B **48** 1
[7] Balashova L L, Grankina T V, Kabachnik N M and Pokhil G P 1990 *Nucl. Instrum. Methods* B **48** 156
[8] Khokonov M Kh and Nitta H 1990 *Phys. Status Solidi* b **159** 589
[9] Shikama T and Nitta H 1990 *Phys. Lett.* **149A** 291
[10] Balashova L L, Kabachnik N M and Kondratyev V N 1990 *Phys. Status Solidi* b **161** 113
[11] Balashova L L, Kondratyev V N and Kabachnik N M 1990 *Nucl. Instrum. Methods* B **48** 18
[12] Robinson M T 1969 *Phys. Rev.* **179** 327
[13] Kumakhov M A and Komarov F F 1981 *Energy Loss and Ion Ranges in Solids* (New York: Gordon and Breach)
[14] Lenkeit K, Trikalinos Ch, Balashova L L, Kabachnik N M and Shulga V I 1990 *Phys. Status Solidi* b **161** 513
[15] Lindhard J 1965 *K. Danske Vidensk. Selsk. Mat.-Fys. Meddr.* **34** 14
[16] Erginsoy C 1965 *Phys. Rev. Lett.* **15** 360
[17] Kumakhov M A and Schirmer G 1980 *Atomnye Stolknovenija v Kristallakh* (Moscow: Atomizdat)
[18] Bohr N 1948 *K. Danske Vidensk. Selsk. Mat.-Fys. Meddr.* **18** 8
[19] Raccah P M, Euwema R N, Stukel D J and Collins T C 1970 *Phys. Rev.* B **21** 756
[20] Lindhard J and Winther A 1964 *K. Danske Vidensk. Selsk. Mat.-Fys. Meddr.* **34** 4
[21] Kabachnik N M, Kondratyev V N and Chumanova O V 1988 *Phys. Status Solidi* b **145** 103
[22] Sung C C and Ritchie R H 1983 *Phys. Rev.* A **28** 674
[23] Esbensen H *et al* 1978 *Phys. Rev.* B **18** 1039
[24] Bulgakov Yu V and Shulga V I 1976 *Radiat. Eff.* **28** 15
[25] Armstrong D D, Gibson W M and Wegner H E 1971 *Radiat. Eff.* **11** 241
[26] Armstrong D D, Gibson W M, Goland A, Golovchenko J A, Levesque R A, Meek R L and Wegner H E 1972 *Radiat. Eff.* **12** 143
[27] Zhukova Yu N, Iferov G A, Tulinov A F and Chumanov V Ya 1972 *Zh. Eksp. Teor. Fiz.* **63** 217

[28] Kadmensky A G and Tulinov A F 1981 *Proc. 7th Int. Conf. on Atomic Collisions in Solids (Moscow 1977)* (Moscow: Moscow State University Publishing House) p 52
[29] Rosner J S, Gibson W M, Golovchenko J A, Goland A N and Wegner H E 1978 *Phys. Rev.* B **18** 1066
[30] Golovchenko J A 1976 *Phys. Rev.* B **13** 4672
[31] Kudrin V V and Vorobiev S A 1975 *Radiat. Eff.* **25** 119
[32] Schiebel U, Neufert A and Clausnitzer G 1976 *Radiat. Eff.* **29** 57